

Microscopic mechanism of electron transfer through the hydrogen bonds between carboxylated alkanethiol molecules connected to gold electrodes

Yang Li, Xingchen Tu, Minglang Wang, Hao Wang, Stefano Sanvito, and Shimin Hou

Citation: *The Journal of Chemical Physics* **141**, 174702 (2014); doi: 10.1063/1.4900511

View online: <http://dx.doi.org/10.1063/1.4900511>

View Table of Contents: <http://scitation.aip.org/content/aip/journal/jcp/141/17?ver=pdfcov>

Published by the [AIP Publishing](#)

Articles you may be interested in


Publisher's Note: "Microscopic mechanism of electron transfer through the hydrogen bonds between carboxylated alkanethiol molecules connected to gold electrodes" [*J. Chem. Phys.* **141**, 174702 (2014)]
J. Chem. Phys. **141**, 199901 (2014); 10.1063/1.4902413

Spin-filtering effect in the transport through a single-molecule magnet Mn 12 bridged between metallic electrodes
J. Appl. Phys. **105**, 07E309 (2009); 10.1063/1.3072789

Electron transport through single conjugated organic molecules: Basis set effects in ab initio calculations
J. Chem. Phys. **127**, 144107 (2007); 10.1063/1.2770718




Contact atomic structure and electron transport through molecules
J. Chem. Phys. **122**, 074704 (2005); 10.1063/1.1851496

Intermolecular effect in molecular electronics
J. Chem. Phys. **122**, 044703 (2005); 10.1063/1.1825377



AIP | The Journal of
Chemical Physics

Meet The New Deputy Editors

	Peter Hamm		David E. Manolopoulos		James L. Skinner
---	-------------------	---	------------------------------	---	-------------------------

Microscopic mechanism of electron transfer through the hydrogen bonds between carboxylated alkanethiol molecules connected to gold electrodes

Yang Li,¹ Xingchen Tu,¹ Minglang Wang,¹ Hao Wang,¹ Stefano Sanvito,² and Shimin Hou^{1,a)}

¹Centre for Nanoscale Science and Technology, Key Laboratory for the Physics and Chemistry of Nanodevices, Department of Electronics, Peking University, Beijing 100871, China

²School of Physics, AMBER and CRANN Institute, Trinity College, Dublin 2, Ireland

(Received 17 August 2014; accepted 15 October 2014; published online 3 November 2014; publisher error corrected 6 November 2014)

The atomic structure and the electron transfer properties of hydrogen bonds formed between two carboxylated alkanethiol molecules connected to gold electrodes are investigated by employing the non-equilibrium Green's function formalism combined with density functional theory. Three types of molecular junctions are constructed, in which one carboxyl alkanethiol molecule contains two methylene, $-\text{CH}_2$, groups and the other one is composed of one, two, or three $-\text{CH}_2$ groups. Our calculations show that, similarly to the cases of isolated carboxylic acid dimers, in these molecular junctions the two carboxyl, $-\text{COOH}$, groups form two H-bonds resulting in a cyclic structure. When self-interaction corrections are explicitly considered, the calculated transmission coefficients of these three H-bonded molecular junctions at the Fermi level are in good agreement with the experimental values. The analysis of the projected density of states confirms that the covalent Au-S bonds localized at the molecule-electrode interfaces and the electronic coupling between $-\text{COOH}$ and S dominate the low-bias junction conductance. Following the increase of the number of the $-\text{CH}_2$ groups, the coupling between $-\text{COOH}$ and S decreases deeply. As a result, the junction conductance decays rapidly as the length of the H-bonded molecules increases. These findings not only provide an explanation to the observed distance dependence of the electron transfer properties of H-bonds, but also help the design of molecular devices constructed through H-bonds. © 2014 AIP Publishing LLC. [<http://dx.doi.org/10.1063/1.4900511>]

I. INTRODUCTION

Understanding electron transport at the single molecule level is the first step to the design of molecular electronic devices in which individual molecules are used as functional active component.^{1,2} Organic molecules are always wired to the metal electrodes through some appropriate linking groups. For example, the thiol group is often used to connect molecules to gold electrodes due to the formation of strong Au-S polar covalent bonds.^{3,4} Recent experiments reveal that long-range non-covalent interactions such as the π - π interaction and the hydrogen bond also play an important role in the formation and the electronic transport properties of molecular devices.⁵⁻⁷ Nishino *et al.* investigated experimentally electron transfer (ET) through the hydrogen bonds formed between two carboxylated alkanethiol molecules respectively connected to one gold electrode,⁷ and found a pronounced dependence of the ET on the molecule lengths. In detail, a H-bond conducts electrons better than a covalent σ bond at short range; however, its conductance decays rapidly as the ET path becomes longer. Since H-bonds are ubiquitous in both artificial and biological systems, many theoretical studies are devoted to understanding the nature of H-bonding.⁸⁻¹² However,

most previous studies focus on the atomic structures and the interaction energies of H-bonding, and rather little is known about their mechanism for ET.

In order to address this issue, here we investigate the atomic structure and the electronic transport properties of H-bonds between two carboxylated alkanethiol molecules by employing the non-equilibrium Green's function (NEGF) formalism combined with density functional theory (DFT), i.e., the NEGF+DFT approach.¹³⁻²² Considering that in experiments ω -carboxyl alkanethiols ($\text{HS}-(\text{CH}_2)_n-\text{COOH}$, which we will denote by SC_nCOOH) with different molecular lengths and gold are respectively employed as the central molecules and the electrode material,⁷ we construct three types of H-bonded molecular junctions. In these one carboxyl alkanethiol molecule is chosen as the SC_2COOH incorporating two methylene ($-\text{CH}_2$) groups and the other carboxyl alkanethiol molecule is composed of one, two or three $-\text{CH}_2$ groups. Our calculations show that, just as the cases of isolated carboxyl acid dimers, the two carboxyl groups in these three molecular junctions also form two H-bonds leading to a cyclic structure. When the self-interaction contained in approximate density functional is treated explicitly, the calculated values of the low-bias junction conductance agree well with the experimentally measured values, illustrating the important effects of the length of the H-bonded molecules on the ET properties of hydrogen bonds.

^{a)} Author to whom correspondence should be addressed. Electronic mail: smhou@pku.edu.cn.

II. CALCULATION METHOD

In this work we use the SIESTA code²³ to compute the atomic structure of molecular junctions formed by carboxylated alkanethiol molecules through H-bonding and the quantum transport code SMEAGOL^{20–22} to study their electronic transport properties. SIESTA is an efficient DFT package, which makes use of improved Troullier–Martins pseudopotentials for describing the atomic cores and adopts a finite-range numerical orbital basis set to expand the wave functions of the valence electrons.^{23,24} While a double-zeta plus polarization (DZP) basis set is used for H, C, O, and S, two different types of basis functions are used for Au, respectively, in the bulk and at the surface. In more detail, a DZP basis set is used for the surface Au atoms, while a single-zeta plus polarization (SZP) basis is used for the bulk. The exchange-correlation functional is at the level of both the generalized gradient approximation (GGA) within the Perdew–Burke–Ernzerhof (PBE) formulation and van der Waals density functional (vdW-DF).^{25–27} Geometry optimization is performed by standard conjugate gradient relaxation until the atomic forces are smaller than 0.03 eV \AA^{-1} . For comparison, all-electron calculations for isolated acetic acid molecules and their dimers are also carried out using both the PBE GGA functional and the MP2 method with the Gaussian 03 code.^{28,29} Here, the 6-311++G(3df,3pd) basis sets are used for hydrogen, carbon, and oxygen atoms.³⁰

SMEAGOL is a practical implementation of the NEGF+DFT approach, which employs SIESTA as the DFT platform.^{20–22} We use an equivalent cutoff of 200 Ry for the real space grid. The charge density is integrated over 32 energy points along the semi-circle, 32 along the line in the complex plane, while 32 poles are used for the Fermi function (the electronic temperature is 25 meV). We always consider periodic boundary conditions in the plane transverse to the transport. The unit cell of the extended molecule comprises ten Au(111) atomic layers with a (3×3) in plane supercell and two carboxylated alkanethiol molecules. The total transmission coefficient $T(E)$ of the junction is evaluated as

$$T(E) = \frac{1}{\Omega_{2DBZ}} \int_{2DBZ} T(\vec{k}; E) d\vec{k}, \quad (1)$$

where Ω_{2DBZ} is the area of the two-dimensional Brillouin zone (2DBZ) in the transverse directions. The k -dependent transmission coefficient $T(\vec{k}; E)$ is obtained as

$$T(\vec{k}, E) = \text{Tr}[\Gamma_L G_M^R \Gamma_R G_M^{R+}], \quad (2)$$

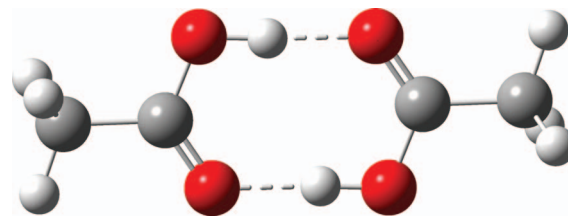


FIG. 1. The optimized atomic structure of the acetic acid dimer in the gas phase.

where G_M^R is the retarded Green's function matrix of the extended molecule and Γ_L (Γ_R) is the broadening function matrix describing the interaction of the extended molecule with the left-hand (right-hand) side electrode. Here, we calculate the transmission coefficient by sampling 4×4 k-points in the transverse 2DBZ.

III. RESULTS AND DISCUSSION

We start our investigations from the atomic structure of the carboxylic acid dimers formed through H-bonding interactions. Taking acetic acid as the representative, the optimized atomic structure of the acetic acid dimer is shown in Fig. 1. As we can see, the most stable dimer configuration is a cyclic structure in which the two carboxyl, $-\text{COOH}$, groups form two strong H-bonds. The lengths of some typical bonds of the isolated acetic acid and the dimer are listed in Table I. When compared with the corresponding experimental value (2.680 \AA),³¹ the hydrogen bond length $\text{O}-\text{H} \cdots \text{O}$ optimized using the vdW-DF functional is underestimated by 0.034 \AA . Although the bond lengths of the $\text{C}=\text{O}$ double bond and the $\text{C}-\text{O}$ single bond in the carboxyl group are both overestimated, which is a known drawback of the vdW-DF functional,³² the lengthening of the $\text{C}=\text{O}$ double bond and the shortening of the $\text{C}-\text{O}$ single bond due to the formation of H-bonds are both predicted correctly. The binding energy is calculated to be 0.67 eV , in good agreement with the benchmark value (0.68 eV) calculated at the CCSD(T)/CBS level.¹² This notation indicates that the level of electron correlation includes contributions evaluated using a coupled-cluster approach through perturbative triple excitations with a complete basis set (CBS) extrapolation. In contrast, the H-bonding interactions are significantly overestimated and the hydrogen bond length $\text{O}-\text{H} \cdots \text{O}$ is only 2.525 \AA , when the PBE GGA functional is employed in the SIESTA code. Although the performance of the PBE GGA functional is improved somewhat when the much larger all-electron 6-311++G(3df, 3pd) basis is used, the optimized hydrogen bond length $\text{O}-\text{H} \cdots \text{O}$ is

TABLE I. Optimized lengths of some typical bonds in the isolated acetic acid molecule and the dimer calculated with Siesta and Gaussian03. The experimental values are also given for comparison.

Bond	Expt. ^a		vdW-DF		PBE/Siesta		PBE/G03		MP2	
	Mol	dimer	Mol	dimer	Mol	dimer	Mol	dimer	Mol	dimer
C=O (Å)	1.214	1.231	1.236	1.259	1.228	1.259	1.213	1.238	1.207	1.226
C–O (Å)	1.364	1.334	1.398	1.354	1.382	1.321	1.366	1.321	1.354	1.319
O–H \cdots O (Å)		2.680		2.646		2.525		2.609		2.646

^aReference 31.

still much shorter than the experimental value. The situation improves dramatically at the MP2/6-311++G(3df,3pd) level, where the calculated bond lengths of these selected bonds are all much closer to the experimental values, in agreement with the well-known results that accurate non-covalent interactions can be predicted by wavefunction theory if a sufficient level of electron correlation is included and a sufficiently large basis set is employed.¹⁰ Considering that the hydrogen bond length and the binding energy calculated at the vdW-DF/DZP level are in good agreement respectively with those calculated at the MP2/6-311++G(3df,3pd) level and the CCSD(T)/CBS level, we can conclude that the vdW-DF functional implemented in the SIESTA code is suitable for the investigations of H-bonding interactions.³³

Next we move our attention to the ET properties of H-bonds. According to the experiment carried out by Nishino *et al.*,⁷ we construct three types of Au-SC_nCOOH//SC₂COOH-Au molecular junctions in which the number of the -CH₂ groups in the first SC_nCOOH molecule is 1, 2, and 3. For the sake of brevity, these three junctions are denoted as the 1-2, 2-2, and 3-2. The atomic structure of the 2-2 junction is shown in Fig. 2(a), which is optimized by using the vdW-DF functional. Just as the cases of isolated carboxyl

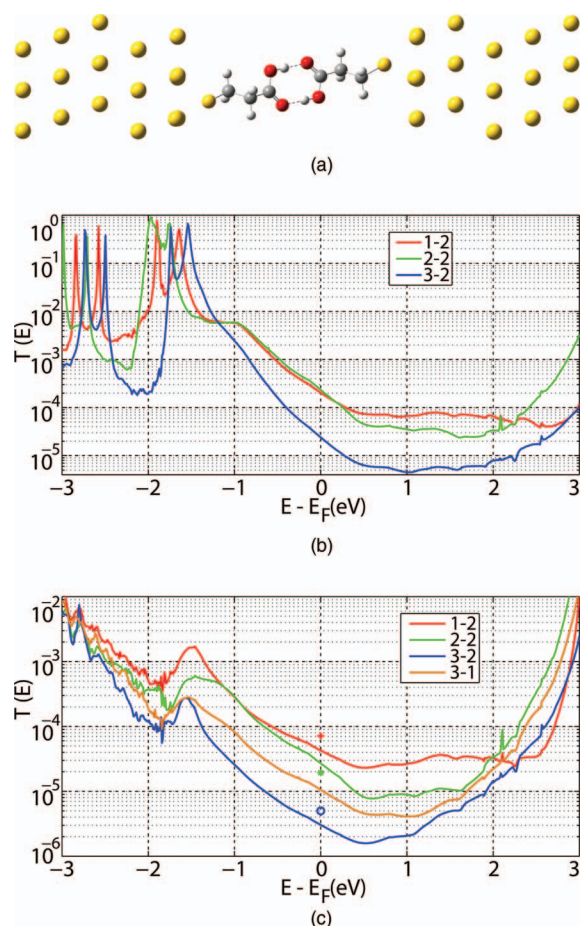


FIG. 2. (a) The atomic structure of the 2-2 molecular junction optimized using the vdW-DF functional, (b) the equilibrium transmission spectra of the 1-2, 2-2, and 3-2 junctions calculated using the PBE GGA functional, (c) the equilibrium transmission spectra of the 1-2, 2-2, 3-2, and 3-1 junctions calculated using the ASIC approach, where the three marks give the experimental values of the 1-2, 2-2, and 3-2 junctions.

acid dimers, the two carboxyl groups in the 2-2 junction also form two H-bonds resulting in a cyclic structure. However, the chemisorption of the SC₂COOH molecule on the Au(111) surface makes the two H-bonds different and their lengths are, respectively, optimized to be 2.659 Å and 2.672 Å. Similar geometric structures are obtained for the other two junctions 1-2 and 3-2, the hydrogen bond lengths are, respectively, calculated to be 2.732 Å and 2.722 Å for the 1-2 junction and 2.740 Å and 2.715 Å for the 3-2 junction. It should be noted that the hydrogen bond lengths in the 1-2 and 3-2 junctions are slightly more elongated than those in the 2-2 junction, compared to the calculated H-bonds in the corresponding isolated dimers (2.634 Å in SC₂COOH//SC₂COOH, 2.656 Å and 2.686 Å in SC₁COOH//SC₂COOH, 2.650 Å and 2.645 Å in SC₃COOH//SC₂COOH). These differences are mainly caused by the construction details of the junction models, especially the distance between the two gold electrodes. Therefore, the hydrogen bonds in the 1-2 and 3-2 junctions are more stretched than those in the 2-2 junction.

Since, as expected, the electronic structures obtained with the vdW-DF functional are essentially the same as those computed with PBE GGA,³⁴ we calculate the transmission spectra of these three molecular junctions at the PBE GGA level (Fig. 2(b)). At the Fermi level, E_F , the transmission coefficients of the 1-2, 2-2, and 3-2 junctions are, respectively, calculated to be 2.0×10^{-4} , 2.3×10^{-4} , and 2.4×10^{-5} , much larger than the corresponding measured values of 7.2×10^{-5} , 1.9×10^{-5} , and 5.0×10^{-6} .⁷ Even worse, the calculated low-bias conductance of the 2-2 junction is unphysically higher than that of the 1-2 junction. However, at energies higher than 0.18 eV above E_F the transmission of the 1-2 junction becomes the largest while that of the 3-2 junction becomes the smallest, which agrees qualitatively with the experimental trend for ET through H-bonds. We note that the transmission around the Fermi level originates from the tail of some transmission peaks located in the energy range of -2.0 eV to -1.5 eV (taken from E_F). It is well known that the molecular levels calculated by using local or semi-local exchange and correlation functionals are usually too high in energy due to the self-interaction error.⁹ Therefore, we infer that the discrepancy between our PBE-calculated low-bias conductance and the experimental results may originate from the incorrect alignment of molecular levels with respect to the electrode Fermi level, which is caused by the self-interaction error contained in the PBE GGA functional.

In the literature several theoretical approaches including the GW approximation (G: the single-particle Green function, W: the dynamic screened interaction function), the DFT+ Σ method and the atomic self-interaction correction (ASIC) scheme have been developed to deal with the alignment problem.³⁵⁻⁴¹ Considering that the GW approximation demands a very high computational cost and that the DFT+ Σ method is currently restricted to molecular junctions in which the molecule remains intact upon adsorption onto the electrode surfaces, here we employ the ASIC method to discuss the effects that self-interaction corrections may have on the calculated ET properties of H-bonds.³⁹⁻⁴¹ The ASIC corrections are only applied to H, C, O, and S atoms in the SC_nCOOH molecules, but not to Au in the electrodes as the

self-interaction error for metals is small. The empirical scale factor α , which is a measure of the deviation of the ASIC potential from the exact SIC one, is set to be 0.70, thus that the highest occupied molecular orbital (HOMO) of the SC_2COOH molecule in the gas phase can be shifted downward to -8.68 eV (i.e., it is much close to the negative of the ionization potential (8.69 eV) calculated at the PBE/PBE/6-311++G(3df,3pd) level). The transmission spectra of the 1-2, 2-2, and 3-2 junctions calculated with the ASIC approach are presented in Fig. 2(c). As we can see, around the Fermi level these transmission spectra now show the correct behavior, that is, the transmission decreases quickly following the increase of the number of the $-\text{CH}_2$ groups contained in the SC_nCOOH molecules. At the Fermi level the transmission coefficients of the 1-2, 2-2, and 3-2 junctions are, respectively, calculated to be 4.3×10^{-5} , 2.7×10^{-5} , and 3.0×10^{-6} , which are in good agreement with the corresponding experimental values⁷ and the errors are never larger than 43%. It should be noted that, compared with the corresponding measured conductance values, the calculated low-bias conductance of the 1-2 and 3-2 junctions are underestimated whereas the calculated conductance of the 2-2 junction is overestimated. This might be caused by the slightly larger hydrogen bond lengths in the 1-2 and 3-2 junctions.

The transmission around the Fermi level is still determined by the tail of the transmission peak located at about -1.5 eV. At variance with the transmission peaks in the energy range of -2.0 eV to -1.5 eV calculated with the PBE functional, which have a peak value approaching unity but a molecule-dependent position (see Fig. 2(b)), the transmission peaks calculated with the ASIC scheme are all positioned at about -1.5 eV. Their peak values are much smaller and decrease rapidly as the central molecule becomes longer. An in-depth insight can be obtained by analyzing the projected density of states (PDOS) of the SC_nCOOH molecules in the junction. Taking the 2-2 junction as an example, the PDOS of the sulfur atom, the two $-\text{CH}_2$ groups and the $-\text{COOH}$ group in one of the two SC_2COOH molecules are shown in Fig. 3. Clearly, the PDOS peak at about -1.5 eV and the PDOS around the Fermi level are both dominated by S. For the $-\text{CH}_2$ and the $-\text{COOH}$ groups, their contributions to the PDOS in this energy range decrease rapidly as the distance between them and the S atom increases, demonstrating that their coupling to S also decreases quickly with distance. The

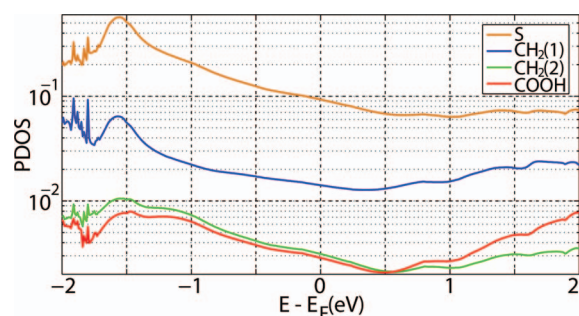


FIG. 3. PDOS of the sulfur atom, the two $-\text{CH}_2$ groups and the $-\text{COOH}$ group in one of the two C_2COOH molecules in the 2-2 junction calculated using the ASIC approach, where the $\text{CH}_2(1)$ group is closer to the sulfur atom than the $\text{CH}_2(2)$ group.

same phenomena are also observed in the 1-2 and 3-2 junctions. It has been shown for alkanethiol molecules assembled on the gold substrate that electronic states near the Fermi level are derived from the covalent bonding between the sulfur atom in the thiol group and the surface gold atoms. For example, an occupied state at -1.4 eV is observed for the octanethiol molecule adsorbed on the Au(111) surface with the standing-up phase.⁴² Therefore, in these 1-2, 2-2, and 3-2 junctions the PDOS peak at about -1.5 eV can also be attributed to the covalent Au-S bonds. Because the Au-S bonds are localized at the Au- SC_nCOOH interfaces, the junction conductance is related to the interaction between the sulfur atom and the $-\text{COOH}$ group which is mediated by the $-\text{CH}_2$ groups in between. As the number of the $-\text{CH}_2$ groups is increased, the coupling between the $-\text{COOH}$ group and S is weakened quickly, resulting in the rapid decrease of the junction conductance. In order to further test this interpretation, we construct another H-bonded junction model in which a SC_3COOH molecule is connected to a SC_1COOH molecule through two H-bonds (i.e., the 3-1 junction). By construction, the hydrogen bond lengths in the 1-3 junction are optimized to be 2.623 Å and 2.643 Å, indicating that the H-bonding interaction in the 1-3 junction is stronger than that in the 2-2 junction. Although the number of $-\text{CH}_2$ groups is the same in the 2-2 and 3-1 junctions, the calculated transmission coefficient at E_F of the 3-1 junction is less than that of the 2-2 junction due to the much weaker coupling between the $-\text{COOH}$ group and S in the SC_3COOH molecule (Fig. 2(c)), confirming the proposed conducting mechanism of ET through H-bonds.

Since the ASIC corrections play a decisive role in the calculations of the transmission spectra of H-bonded molecular junctions, we finally explore how the self-interaction affects their calculated transport properties (taking the 2-2 junction as the representative). This is realized by tuning gradually the empirical scale factor α from zero to the final value of 0.7. The larger the α value is, the less the self-interaction error is contained in the approximate DFT exchange-correlation functional. When the scale factor α is set to zero, i.e., the Perdew-Zunger (PZ) local density approximation (LDA) functional is used,⁴³ the transmission spectrum of the 2-2 junction is almost identical to that obtained with the PBE GGA functional, showing a double-peak structure at around -1.8 eV together with a small shoulder at about -1.0 eV (Fig. S1 in the supplementary material).⁴⁴ The PDOS analysis confirms that this transmission doublet is dominated by the $-\text{COOH}$ group and that the shoulder is mainly contributed by the S atom. Eigenchannel analysis^{45,46} reveals that the double-peak structure is mainly contributed by some p-type orbitals of the two oxygen atoms forming the C=O double bonds, which form a $\text{pp}\sigma$ conducting channel connecting the two $-\text{COOH}$ groups (Fig. S2 in the supplementary material).⁴⁴ Following the increase of the scale factor α , the double-peak structure dominated by the $-\text{COOH}$ groups rapidly shifts downwards in energy and moves below -3.0 eV for $\alpha = 0.5$ (Fig. S3 in the supplementary material).⁴⁴ In contrast, the downward shift of the transmission shoulder is much slower: when α increases from 0 to 0.7, it is only shifted from -1.0 eV to -1.5 eV and dominates the transmission around the Fermi level. Therefore, compared to the transmission spectra obtained with the

PBE GGA and PZ LDA functionals, the ASIC corrections remove the spurious contributions of the $-\text{COOH}$ groups to the transmission around the Fermi level. Thus the Au-S bonds localized at the Au- SC_nCOOH interfaces and the coupling between the $-\text{COOH}$ group and the S atom become the critical factors determining the low-bias conductance of the H-bonded Au- $\text{SC}_n\text{COOH}/\text{SC}_2\text{COOH}$ -Au junctions.

IV. CONCLUSION

We have investigated the atomic structure and the electronic transport properties of hydrogen bonds formed between two carboxylated alkanethiol molecules connected to gold electrodes by means of the NEGF+DFT approach. Our calculations show that, similarly to the cases of isolated carboxylic acid dimers, in the Au- $\text{SC}_n\text{COOH}/\text{SC}_2\text{COOH}$ -Au molecular junctions ($n = 1, 2, 3$) two H-bonds are also formed between the two carboxyl groups and thus they are in a cyclic structure. When the self-interaction corrections are taken into account explicitly, the calculated transmission coefficients of these three H-bonded molecular junctions at the Fermi level are well consistent with the measured values. PDOS analysis confirms that the low-bias junction conductance originates from the covalent Au-S bonds localized at the molecule-electrode interfaces. Since the coupling between the $-\text{COOH}$ group and the sulfur atom is weakened by the $-\text{CH}_2$ groups in between, the junction conductance decays rapidly as the ET pathway becomes longer. Further investigations on the ET properties of the H-bonds between conjugated molecules functionalized with the $-\text{COOH}$ groups will be carried out in the future, with the emphasis on whether the H-bonds have more direct effects on the low-bias junction conductance. Our findings will help the design of molecular devices constructed through hydrogen bonds.

ACKNOWLEDGMENTS

This project was supported by the National Natural Science Foundation of China (No. 61321001) and the MOST of China (Nos. 2011CB933001 and 2013CB933404). S.S. thanks additional funding support from the European Research Council (QUEST project), by KAUST (FIC/2010/08) and by AMBER (12/RC/2278).

¹N. J. Tao, *Nat. Nanotechnol.* **1**, 173 (2006).

²H. Song, M. A. Reed, and T. Lee, *Adv. Mater.* **23**, 1583 (2011).

³M. A. Reed, C. Zhou, C. J. Muller, T. P. Burgin, and J. M. Tour, *Science* **278**, 252 (1997).

⁴H. Song, Y. Kim, Y. H. Jang, H. Jeong, M. A. Reed, and T. Lee, *Nature (London)* **462**, 1039 (2009).

⁵S. Wu, M. T. González, R. Huber, S. Grunder, M. Mayor, C. Schönberger, and M. Calame, *Nat. Nanotechnol.* **3**, 569 (2008).

⁶S. V. Aradhya, M. Frei, M. S. Hybertsen, and L. Venkataraman, *Nature Mater.* **11**, 872 (2012).

⁷T. Nishino, N. Hayashi, and P. T. Bui, *J. Am. Chem. Soc.* **135**, 4592 (2013).

⁸S. Scheiner, *Hydrogen Bonding: A Theoretical Perspective* (Oxford University Press, New York, 1997).

⁹W. Koch and M. C. Holthausen, *A Chemist's Guide to Density Functional Theory*, 2nd ed. (Wiley-VCH, Weinheim, 2000).

¹⁰M. S. Marshall, L. A. Burns, and C. D. Sherrill, *J. Chem. Phys.* **135**, 194102 (2011).

¹¹K. S. Thanthiriwatte, E. G. Hohenstein, L. A. Burns, and C. D. Sherrill, *J. Chem. Theory Comput.* **7**, 88 (2011).

¹²G. A. Dilabio, E. R. Johnson, and A. Otero-de-la-Roza, *Phys. Chem. Chem. Phys.* **15**, 12821 (2013).

¹³Y. Meir and N. S. Wingreen, *Phys. Rev. Lett.* **68**, 2512 (1992).

¹⁴P. Hohenberg and W. Kohn, *Phys. Rev.* **136**, B864 (1964).

¹⁵W. Kohn and L. J. Sham, *Phys. Rev.* **140**, A1133 (1965).

¹⁶Y. Xue, S. Datta, and M. A. Ratner, *Chem. Phys.* **281**, 151 (2002).

¹⁷M. Brandbyge, J.-L. Mozos, P. Ordejón, J. Taylor, and K. Stokbro, *Phys. Rev. B* **65**, 165401 (2002).

¹⁸J. Zhang, S. Hou, R. Li, Z. Qian, R. Han, Z. Shen, X. Zhao, and Z. Xue, *Nanotechnology* **16**, 3057 (2005).

¹⁹R. Li, J. Zhang, S. Hou, Z. Qian, Z. Shen, X. Zhao, and Z. Xue, *Chem. Phys.* **336**, 127 (2007).

²⁰A. R. Rocha, V. M. Garcia-Suarez, S. W. Bailey, C. J. Lambert, J. Ferrer, and S. Sanvito, *Nature Mater.* **4**, 335 (2005).

²¹A. R. Rocha, V. M. Garcia-Suarez, S. Bailey, C. Lambert, J. Ferrer, and S. Sanvito, *Phys. Rev. B* **73**, 085414 (2006).

²²I. Rungger and S. Sanvito, *Phys. Rev. B* **78**, 035407 (2008).

²³J. M. Soler, E. Artacho, J. D. Gale, A. García, J. Junquera, P. Ordejón, and D. Sánchez-Portal, *J. Phys.: Condens. Matter* **14**, 2745 (2002).

²⁴N. Troullier and J. Martins, *Phys. Rev. B* **43**, 1993 (1991).

²⁵J. Perdew, K. Burke, and M. Ernzerhof, *Phys. Rev. Lett.* **77**, 3865 (1996).

²⁶M. Dion, H. Rydberg, E. Schröder, D. C. Langreth, and B. I. Lundqvist, *Phys. Rev. Lett.* **92**, 246401 (2004).

²⁷G. Román-Pérez and J. M. Soler, *Phys. Rev. Lett.* **103**, 096102 (2009).

²⁸M. Head-Gordon, J. A. Pople, and M. J. Frisch, *Chem. Phys. Lett.* **153**, 503 (1988).

²⁹M. J. Frisch, G. W. Trucks, H. B. Schlegel *et al.*, GAUSSIAN 03, Revision C.02, Gaussian, Inc., Pittsburgh, PA, 2003.

³⁰M. J. Frisch, J. A. Pople, and J. S. Binkley, *J. Chem. Phys.* **80**, 3265 (1984).

³¹J. L. Derissen, *J. Mol. Struct.* **7**, 67 (1971).

³²J. Klimeš, D. R. Bowler, and A. Michaelides, *Phys. Rev. B* **83**, 195131 (2011).

³³D. J. Carter and A. L. Rohl, *J. Chem. Theory Comput.* **8**, 281 (2012).

³⁴I. Hamada and S. Yanagisawa, *Phys. Rev. B* **84**, 153104 (2011).

³⁵J. B. Neaton, M. S. Hybertsen, and S. G. Louie, *Phys. Rev. Lett.* **97**, 216405 (2006).

³⁶M. strange, C. Rostgaard, H. Häkkinen, and K. S. Thygesen, *Phys. Rev. B* **83**, 115108 (2011).

³⁷S. Y. Quek, H. J. Choi, S. G. Louie, and J. B. Neaton, *Nano Lett.* **9**, 3949 (2009).

³⁸C. Jin, T. Markussen, and K. S. Thygesen, *Phys. Rev. B* **90**, 075115 (2014).

³⁹C. D. Pemmaraju, T. Archer, D. Sánchez-Portal, and S. Sanvito, *Phys. Rev. B* **75**, 045101 (2007).

⁴⁰C. Toher and S. Sanvito, *Phys. Rev. Lett.* **99**, 056801 (2007).

⁴¹C. Toher and S. Sanvito, *Phys. Rev. B* **77**, 155402 (2008).

⁴²M. Nakaya, M. Shikishima, M. Shibuta, N. Hirata, T. Eguchi, and A. Nakajima, *ACS Nano* **6**, 8728 (2012).

⁴³J. P. Perdew and Z. Zunger, *Phys. Rev. B* **23**, 5048 (1981).

⁴⁴See supplementary material at <http://dx.doi.org/10.1063/1.4900511> for the transmission spectra and the PDOS of the 2-2 junction calculated using the ASIC scheme with different scale factors, and the eigenchannel analysis of the 2-2 junction.

⁴⁵R. Li, S. Hou, J. Zhang, Z. Qian, Z. Shen, and X. Zhao, *J. Chem. Phys.* **125**, 194113 (2006).

⁴⁶M. Paulsson and M. Brandbyge, *Phys. Rev. B* **76**, 115117 (2007).